The Reconstruction and Research Progress of the TEXT-U Tokamak in China

G. Zhuang 1), Y. Pan 1), X.W. Hu 1), Z.J. Wang 1), Y.H. Ding 1), M. Zhang 1), L. Gao 1), X.Q. Zhang 1), Z.J. Yang 1), K.X. Yu 1), K.W. Gentle 2), H. Huang 2), the J-TEXT team 1)

1) College of Electrical and Electronic Engineering, Huazhong University of Science and Technology, Wuhan Hubei, 430074, China

2) Fusion Research Center, University of Texas at Austin, Austin, 78712, USA

E-mail address of the main author: ge.zhuang@mail.hust.edu.cn

Abstract. The TEXT/(TEXT-U) tokamak, formerly built and operated by the University of Texas at Austin in USA, was dismantled and shipped to China in 2004, and renamed as the Joint TEXT (J-TEXT) tokamak. The reconstruction work, which included reassembly of the machine and development of peripheral devices, was completed in spring of 2007. Consequently, the first plasma was obtained at the end of 2007. At present, a typical J-TEXT Ohmic discharge can produce a plasma with flattop current up to 220kA and lasting for 300ms, line averaged density above $2\times10^{19}m^{-3}$, and an electron temperature about 800eV, with a toroidal magnetic field of 2.2T. A number of diagnostic devices used to facilitate the routine operation and experimental scenarios were developed on the J-TEXT tokamak. Hence, the measurements of the electrostatic fluctuations in the edge region and conditional analysis of the intermittent burst events near the last closed flux surface (LCFS) were undertaken. The observation and simple analysis of MHD activity and disruption events were also performed. The preliminary experimental results and the future research plan for the J-TEXT are described in detail.

1. Introduction

In the late 1970s, the University of Texas (UT) at Austin proposed to build a fusion plasma research facility, namely the Texas EXperimental Tokamak (TEXT)[1], which served as a general-purpose device designed for good experimental accessibility and routine operation for fusion experiments committed to specific objectives. In the 1980s, the TEXT was operated by UT at Austin and yielded fruitful results. In the 1990s, a major upgrade to the TEXT (TEXT-U) was planned specifically in an attempt to obtain an H-mode plasma by adding high power electron cyclotron waves to a divertor plasma[2]. In 2004, according to the agreement between UT at Austin and Huazhong University of Science and Technology (HUST), the facility was moved to China, placed on the HUST campus, and renamed as the Joint TEXT (J-TEXT). Thereafter, the reconstruction of the tokamak began, which included on-site construction, reassembly of the machine hardware and a flywheel motor-generator, and design and manufacture of peripheral equipment. All the work was completed in spring of 2007. Meanwhile a few fundamental diagnostic instruments were designed, manufactured, and set up. With support of those diagnostics, the first commissioning commenced in summer of 2007. The reassembled machine and all the developed peripheral systems were successfully tested and adjusted to their optimal working conditions. Consequently, the first plasma was obtained at the end of 2007[3]. The renewed TEXT-U tokamak will play a key role in the universities of China for training young scientists and promoting experimental research in basic plasma physics.

The TEXT/TEXT-U/J-TEXT is a conventional tokamak with an iron core. Its nominal parameters are summarized here: the major radius R=105cm, the minor radius r=25-29cm with a movable titanium-carbide coated graphite limiter, the maximum toroidal field B_T=3T, the maximum plasma current I_p=400kA lasting for 400ms, plasma densities n_e=1-10×$10^{19}m^{-3}$,

and an electron temperature T_e~1keV. The research program on the TEXT/TEXT-U was principally devoted to the study of plasma transport and turbulence[4], in particular to understanding the role of turbulence. A survey of interior and edge turbulence characteristics had been completed. Since the machine has flexibility and good accessibility for diagnostics development, a great effort to develop advanced diagnostics devices had been made. For example, in order to identify the local transport process, both adequate profile diagnostics and a unique complement of interior fluctuation diagnostics were set up, such as far infrared (FIR) collective scattering, heavy-ion beam probe, etc.

Now, the J-TEXT operates in an Ohmic heating regime with a limiter. The operating behavior and limits are understandable and reasonable of the machine. Using the limited diagnostic tools, some experimental research topics are being studied on the machine. For example, observation of MHD activity and measurements of the electrostatic fluctuations are undertaken. The preliminary results are described in the following sections.

2. Reconstruction of the TEXT-U tokamak

In the preceding step of reconstruction, the on-site construction work on the HUST campus, which comprises the foundations, heat exchangers, alterations of the old laboratory, crane, and so on, had to be specified, designed and completed for installation. The reconstruction as shown in figure 1 can be divided into two major categories. One was integration of the flywheel motor-generator and development of its peripheral equipment, which includes water cooling system, heat exchanger, and oil supply system, etc. The other one was to assemble the tokamak. This work not only includes the combination of all the hardware of the machine, such as iron core, torus, field coils and their support frame and force structures, but also involved design and development of new peripheral systems, such as pumping stations and gas puffing systems, field coil power supplies, water cooling and deionized system, central control system (CCS), data acquisition and management (DAQ) system, a number of routine diagnostic systems, and so on. All the reconstruction work has completed in spring of 2007. Facility hookup and preliminary operational checkout was completed in fall of 2007.

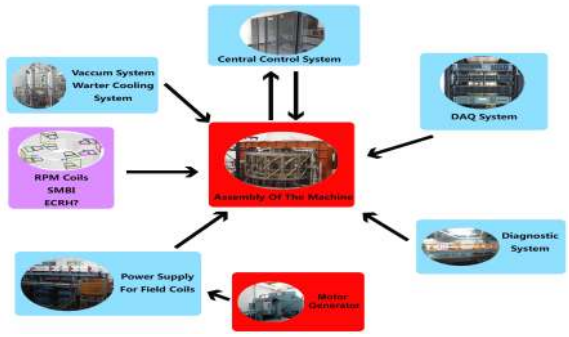

Fig. 1. The schematic of the reconstruction work of the J-TEXT, where the 'red block' means the assembly of the shipped hardwares (including the machine and the flywheel motor-generator), the 'blue block' denotes the newly developed systems and devices, the 'purple block' indicates the projects in the future plan.

2.1. Design and setup of the vacuum system

The J-TEXT vessel has a total volume of 3.2m^3 and its surface area is about 18m^2. The vessel is formed in two halves, joined by two keystones that included insulating breaks. Most of the inner wall surface is covered by the graphite tiles. Due to the sealing materials of the vessel, the design bake-out temperature is limited to 100^{o}C. The new vacuum system[5] consists of two pumping stations, two types of discharge cleaning systems, two sets of gas puffing systems, and a number of gauges. Each pumping station consists of a forepump, a turbo-molecular pump and a cryopump. With the effective pumping speed 3m^3/s provided by

two running pumping stations, the rough-down time from air to 10Pa is about 60min, and the pump-down to 1.2×10^{-4}Pa after a shot in hydrogen is less than 3 min. The base pressure inside the vessel can be lowered to 6.6×10^{-6}Pa, which easily satisfies the discharge requirement. Both Taylor discharge cleaning and glow discharge cleaning are used to clean the plasma-facing components inside the vessel to guarantee a good wall condition. Taylor discharge cleaning works as the main cleaning tool with discharge cleaned for 12 hours each night and continuously on weekends. The gas puffing system, which consists of a container and a piezo-electric valve controlled by feedback loop or preset waveforms for rapid modulation, is used to fill Hydrogen or other type of gas to suit the experimental needs. Several types of gauges, covering pressures ranging from atmospheric pressure to 10^{-7}Pa, are currently in use. Vacuum conditions are continually monitored with a residual gas analyzer (RGA) during the operation.

2.2. Modificiation of the field coil power supplies

Because of the grid difference between China (50Hz) and USA (60Hz) and improved electrical technology, the previous magnet power supplies had to be extensively modified especially their control systems.

The toroidal field (TF) coils, cooled by deionized water, consist of 16 nearly round shaped copper coils segments interlinked in series with 6 turns per segment. The TF power supply energized by the 100MW/100MJ flywheel motor-generator can drive a flat current up to 120kA, which generates the TF up to 2.25T [6]. The TF coils produce a toroidal field with an average ripple of less than 1% with a maximum of 3% at the outer edge.

Three separate coil systems are placed toroidally around the torus of J-TEXT to produce different types of poloidal fields (PFs), namely the Ohmic heating (OH) field, the vertical field (VF) and the horizontal field (HF). The OH coil consists of a 40-turn solenoid inductively coupled to the plasma aided by an iron-core transformer with two return legs and has a up-limit flux of 1.6V·s. The OH power supply is the most complex electrical source on the J-TEXT, which comprises one rectifier circuit, one pre-magnetizing circuit, four capacitance-bank discharge circuits, and an ionization capacitance discharge circuit. The system has the capability to provide 10kA current at $300V_{DC}$ within 0.5s interval in the OH coil, which enables plasma currents up to 400kA. The plasma equilibrium is achieved by the functioning of two other PFs composed of a 16-turn VF coil and a 32-turn HF coil, respectively. Both coil systems are driven from the power grid at 380V. The VF power supply can drive a 10kA current at $200V_{DC}$ lasting for 0.5s. The HF power supply is able to feed forward and reverse current to the coils up to 500A in the range of $\pm150V_{DC}$ which lasts for 0.5s [7]. Both VF and HF power supplies are feedback-controlled to maintain plasma position.

2.3. Development of the central control system (CCS)

The novel CCS system developed under a UNIX-style real-time operating system QNX is a multi-mission system that functions as a machine coordinator, discharge pilot, data manager, and emergency response [8]. The system can control all the subsystems and realize some basic functions as follows: (1) Discharge waveform design: the discharge waveforms for the TF, OH, VF, HF, and gas puffing can be carefully aligned to meet the user's demand. (2) Timing sequence control: the timing sequence may be controlled so as to permit each relevant subsystem to engage in the process at the right time, peculiarly to real-time manage all the

magnetic fields to meet the experimental requirements. (3) Status cruise and safety control: the CCS system can check the status of every sub-system at a 1kHz rate and update the security information time to time. If an abnormal event occurs, it can immediately block the discharge sequence and activate contingency plans to protect the subsystems. (4) Post-shot service: This process can be prompted by the plasma current ramp-down and thereby alter the discharge control to the normal waiting status. The services contain system checks, all the subsystem resets, shot-number update, data transfer and archive, etc.

2.4. Development of diagnostic systems

Since the TEXT-U shipment did not contain any diagnostic instruments, a number of fundamental diagnostics had to be designed and developed to assist the first commissioning and then facilitate the daily operation in the early campaign. They take the measurements of: (1) Plasma current: The plasma current is measured with three redundant Rogowski loops poloidally winding around the vessel. Two identical sets of printed circuit board (PCB) Rogowski coils were mounted outside the vessel at two symmetrical toroidal positions. One handmade conventional Rogowski coil was installed inside the vessel. All 3 sets of coils have an insignificant error of a few kiloamps. (2) Loop voltage: Three 1-turn flux loops toroidally winding around the vessel with different locations R=44.6cm, 49.3cm, 106cm respectively, are used to provide the loop voltage. (3) Plasma position: Four sets of PCB magnetic diagnostic coils installed inside the vacuum vessel are used for detecting the plasma radial and vertical displacements. Each coordinate is determined by a pair of variable cross-section Rogowski and saddle coils [9]. (4) Averaged density: A 2mm microwave interferometer system is used for the measurement of center chord line-integrated electron density for the routine operation and for the density feedback control. A bias-tunable Gunn oscillator operating at 150GHz (cutoff density is $2.8\times10^{20}m^{-3}$) with output power of 10mW is employed as a frequency-modulated source. The nominal IF of the system is 100kHz [10]. (5) Hard x-ray emission: Intensity of hard x-ray emission is measured by two sets of fixed scintillation counters away from the torus, viewing tangentially and radially, respectively. The measured results are used to evaluate the strength of runaway electrons. (6) Residual gas: An Inficon RGA is installed on one pumping station to monitor the composition of filling gas (H_2, D_2, and impurities), hence to determine the progress of discharge cleaning and detect contamination in the vessel. (7) Visible light: A wide-viewing-angle visible light imaging system located at a tangential window is designed to monitor the visible light emission from the boundary region, and hereby to monitor the discharge progress [11].

Since 2008, a number of other diagnostic tools have been developed mainly to satisfy the needs of research topics, such as investigation and hence comprehension of various MHD activities, turbulence and transport, and so on. The diagnostic systems now in use are listed as follows: (1) Multichannel FIR interferometer employs seven channels cross the J-TEXT cross-section vertically. Their radial positions are r=21cm, 14cm, 7cm, 0cm, -21cm, -14cm, -7cm, respectively. The laser source is a continuous-wave HCN laser with a wavelength of 337μm (cutoff density is $9.8\times10^{21}m^{-3}$) and an output power up to 100mW. The IF frequency can be adjusted by a rotating grating and is fixed at 10kHz. Both plasma density and fluctuations can be measured. (2) There are two poloidal arrays of 2D Mirnov coils mounted inside the vessel, one array of 24 coils (equivalently located in a circular shape) and the other one of 20 (in a rectangular shape). There is also one toroidal array of 16 coils installed inside the torus. All of them are used to detect external MHD activity and permit determination of (m,n) of the mode. (3) An X-ray pulse height Analyzer (consists of 3 Silicon shift detectors) is used to measure the soft x-ray emission spectrum to determine Te, strong metallic lines, and

the super-thermal electron distribution. It can detect photon energies ranging from 1keV to 20keV, and the low energy photons will be shielded by 8μm beryllium filter. Its temporal resolution is 50ms. (4) Three soft X-ray photodiode arrays mounted at the same toroidal location but different poloidal positions are used to detect soft x-rays. The vertically viewing array consists of 35 detectors which view the entire plasma cross-section. The horizontally viewing array has 2 sets of 35 detectors located ±15 degrees from the mid-plane. The system has a spatial and temporal resolution of 2cm and 4μs, respectively. A 6.5μm beryllium filter is used to restrict the spectral acceptance of the cameras to 0.5-13keV [12]. (5) Three miniature pinhole AXUV16ELG (16 elements absolute extreme ultraviolet silicon photodiodes) array cameras, which are set at the same toroidal position but in three different poloidal places, can provide a broad viewing angle that covers the whole plasma cross section, hence can measure the total radiated power and the radiated emissive profile. The layout is similar to that of soft X-ray arrays. Another nine AXUV10EL (10 elements) array cameras are divided into three groups and mounted at different toroidal locations to observe the toroidal radiated power distribution. The AXUV array has a sensitivity from 0.20 to 0.27A/W for photon energies of 25eV-6keV [13]. (6) The spectrometer with 2400lines/mm grating is used to record the emission spectrum from 200nm to 1100nm along a vertical center chord through the plasma. The integration time of the spectrometer is adjusted to 100ms. Two identical photodiode arrays (PDAs) aiming for visible-light detection with a specified front filter (center 464.7nm, bandwidth 3nm) is designed to record CIII line spectrum, while another (center 656.2nm, bandwidth 3nm) is used for the H_α line. This hardware can be used to measure the impurity transport. (7) Several types of Langmuir probes, capable of measuring up to a few centimeters inside the limiter radius, provide data on electron density and temperature, the floating potential, and fluctuations of these quantities in the boundary region [14].

Moreover, in our plan there are some important and advanced diagnostic instruments to be developed for some specified research topics. For example, a 3-wave FIR interferometer-polarimeter system for current density profile, a multi-channel ECE for electron temperature profile, etc. The layout of the J-TEXT diagnostics is illustrated in Fig. 2.

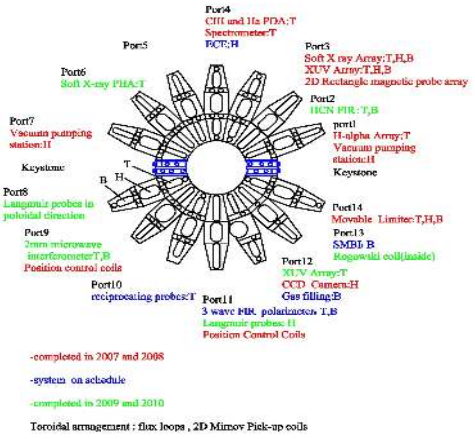

Fig. 2. The layout of the J-TEXT diagnostic systems, where 'T' denotes the top diagnostic window, 'H' the horizontal window, and 'B' the bottom window.

2.5. Construction of the data acquisition and management (DAQ) system

The new DAQ system formed on base of the Redhat Linux Enterprise Operating System and MDSplus database performs various functions as recording, transferring, writing, duplicating, and accessing the measured data.

In daily operation, the data acquisition terminals will record measured signals and then

convert them to digital ones. The Adlink DAQ2205 high-speed multi-channel data acquisition cards with the maximum sampling rate of 50ksps at 16-bit resolution are adopted for low frequency signal acquisition, while the British D-TACQ produced ACQ196 series with the maximum sampling rate of 500ksps at 16-bit resolution for the high-frequency signals. All the digital data is then transmited to the data server via fiber-optic Ethernet and written into the MDSplus tree. Via the fiber optic interface, the data server links to disk array cabinets for data duplication, and also connects to the tape library for data backup. The data service functions are built around the embedded MDSplus toolkit in the data server. A series of powerful solutions provided by MDSplus toolkit can program archive structures, model tree creation and service function design, etc. The MDSplus provides the friendly module/interface for user access to the data. In addition, the WEB server can provide the website navigation and experimental data access as well.

2.6. Operation and performance

A broad range of J-TEXT Ohmic discharge conditions in hydrogen have been catalogued. Discharges can last up to 300 ms except at the highest currents. They are well controlled and reproducible. One discharge takes roughly 80 ms for the current to rise and an equilibrium to established. Then a constant plateau condition can be maintained for 300 ms thereafter. The range of readily-available plasma currents and densities for each of the toroidal fields commonly chosen have been studied.

At present, the limiter configuration of the J-TEXT tokamak is fixed at a major radius R=1.05m and a minor radius a=0.27m. Under the condition of B_T=2.2T and gas prefilling pressure of 0.02Pa, a typical Ohmic discharge achieved in the machine is the production of plasma current of more than 200kA (q_a~3.5) with a flattop duration of 250ms. The V_{loop} decreases from the peak ~25V to less than 2V. Normally, the line averaged density of such discharges exceeds ~$2\times10^{19}m^{-3}$, while the electron temperature is near 800eV. A example is displayed in Fig. 3, which plots plasma current, loop voltage, x and y position, density, and a central Soft X-ray channel showing sawteeth during the plateau.

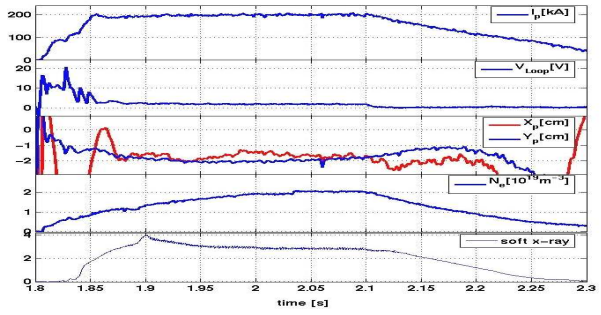

Fig. 3. Traces of a typical Ohmic discharge in J-TEXT (shot 10011674), where the legend 'I_p' denotes plasma current, 'V_{loop}' for loop voltage, 'X_p' and 'Y_p' for x and y position, rescpectively, 'n_e' for density, and 'soft x-ray' for intensity observed by a central Soft X-ray channel

3. Research progress on the J-TEXT

Benefiting from the diagnostic tools that have been developed, experimental studies have emphasized the types of MHD activity and disruptions that occur, and fluctuation and turbulence in the plasma edge region. The preliminary results from those programs are described below.

3.1. Observation and analysis of the intermittent burst events

Many studies have shown that turbulence has a dominant influence in the edge region of the

plasma. Recently, investigation of the turbulence characteristics in the edge region were undertaken in the J-TEXT, especially on the intermittent burst events (IBEs). In order to understand the nature of the IBEs, a rather comprehensive analysis was performed on the Langmuir probe signals obtained in the edge region [14].

The scenarios are carried out under the following conditions: toroidal field B_T=2.2T, plasma current I_p=200kA, and a line-averaged electron density $n_e=1.3\times10^{19}m^{-3}$. The measurements are made using a square probe array, which consists of four carbon tips with each tip 2 mm long and 1 mm in diameter and mounted on the top window of the tokamak. The probe can be moved radially shot-by-shot. Two of the tips are operated as a double probe with a constant bias voltage of 180 V to record the ion saturation current (Is). The other two tips are spaced poloidally to measure the floating potentials. The sampling rate of the signals is 500kHz.

The intermittency of the density fluctuations can be identified by the analysis of the Is signals. Fig. 4 shows an example of the time-varying fluctuations of Is and their corresponding PDFs at three different radial locations, where the fluctuations are normalized by their standard deviation. In figure 4, the positive fluctuations are slightly more than negative ones in the Is signals near the LCFS, while deep into SOL, the fluctuations are dominated by much larger positive peaks. The asymmetry of the PDFs in the SOL increases with increasing radius. Conditional analysis suggests that the IBEs have a significant impact on the radial transport. The fraction of the particle transport carried by the IBEs is about 10-20% around the LCFS.

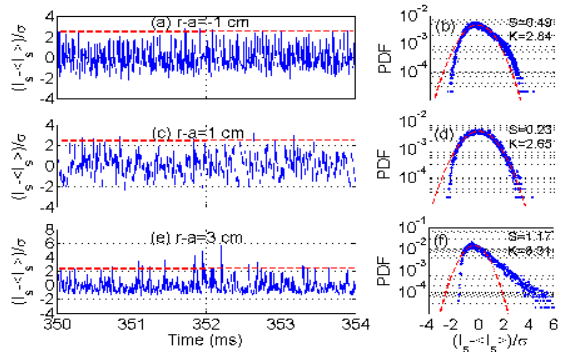

Fig. 4. Time evolution of Is fluctuations normalized by their standard deviations (a, c and e), and the corresponding PDFs (b, d and f) at three different radial locations, respectively. The red dotted lines indicate the amplitudes of the Is fluctuations equal to 2.5 times their deviation (a, c and e) and the best Gaussian fit to the PDFs (b, d and f).

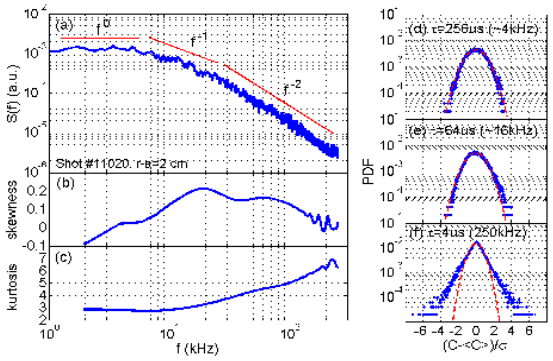

Fig. 5. Power spectrum of the Is fluctuation (a), the dependences of the skewness and kurtosis of the Is fluctuation with frequencies (b and c), and the PDFs of the Is fluctuation at three different frequencies (d, e and f). The red dotted lines indicate the best Gaussian fit to the PDFs (d, e and f).

Meanwhile, a conventional power spectrum of the density fluctuation is obtained by Fourier analysis. There are no obvious peaks in the spectrum shown in Fig. 5(a), implying no periodic fluctuations. The shape of the spectrum can be catalogued into three ranges described by power-law dependences of $S(f)\propto f^{-m}$, as having been presented in other tokamaks. The presence of the m=1 region, gives an indication of the avalanche interactions. Furthermore, the power-law dependences of the spectrum suggest the self-similar behavior of the density fluctuation at three different ranges. Figures 5(b) and 5(c) show the dependences of skewness and kurtosis with frequencies. The skewness has a maximum value near the frequency of f=20kHz, suggesting a maximum positive deviation at this frequency. From 20kHz to 250kHz, the skewness tends to decrease with high frequency. The kurtosis is increasing when the

increasing frequencies above 10kHz, indicating that the intermittency of the density fluctuation is more obvious at high frequencies. In addition, the PDFs of the density fluctuations at the three different power-law regions (represented by different time scales) are near-Gaussian, positive skewed and more stretched, as shown in Fig. 5(d), (e), and (f), respectively, which are in accordance with the skewness and kurtosis calculations.

In order to investigate the dynamic characteristics between successive burst events, the quiet time statistical method is performed on the Is signals. The distribution of the quiet times between all burst events in the system essentially reflects the statistics of the drive. In the analysis, a reference level of 2.5 times deviation of the density fluctuation is used to measure the quiet times between burst events. The PDF of the quiet times is shown in Fig. 6, displaying two distinct power-law regions ($P(\tau) \propto \tau_q^{-\gamma}$) with γ=1.05±0.06 and γ=2.29±0.18, respectively. The result implies the existence of correlation between burst events and possible different dynamics in the two power-law regions.

To improve our understanding of burst effects on transport, two sets of 1-D Langmuir probe arrays were used to measure the propagation of the turbulent structures in the r-θ plane. The preliminary analysis of measured Is signals shows that the structures with higher amplitudes have higher radial and poloidal velocities. Both the radial velocity and the poloidal velocity decrease outward along the radius, as shown in Fig. 7. The radial velocity approaches to the poloidal velocity in the far SOL. The details will be published elsewhere.

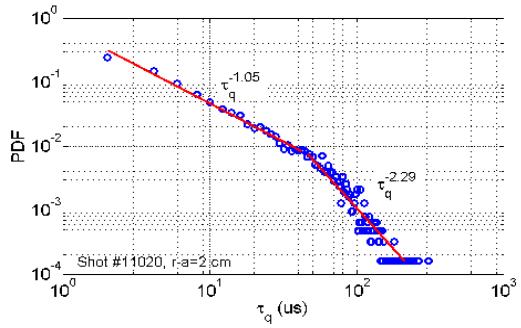

Fig. 6. Probability distribution function of the quiet times. Power law fit is shown by the red solid lines.

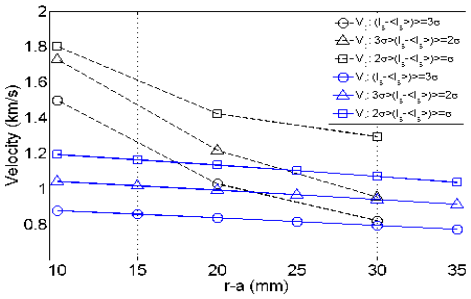

Fig. 7. The radial dependence of the radial and poloidal velocity for different thresholds. Vp: poloidal velocity, Vr: radial velocity.

3.2. Preliminary investigation of disruption events and operation region

Disruptions are as important issue associated with the tokamak fusion reactors and their operations. With the occurrence of the major disruptions, large energy can be poured onto the first wall and divertor plates in very short time and hence may cause large damage to the device. Moreover, large electromagnetic forces induced by eddy and halo currents generated by disruptions can also damage the vacuum vessel and in-vessel components. Therefore it is meaningful to carry out diverse disruption observations in the tokamak to accumulate relevant data for disruption control and mitigation.

In general, there can be several reasons for a major disruption. Some discharge exceed the tokamak operating region referred to the Hugill diagram (An example of the J-TEXT is shown in Fig. 8), which can easily trigger the disruption. This type of disruption can be avoided by setting plasma parameters properly. Nevertheless, some discharges well located within the operation region will also end in the precipitate disruptions, so it is of importance

to scan the plasma conditions for the precursor analysis and damage evaluation.

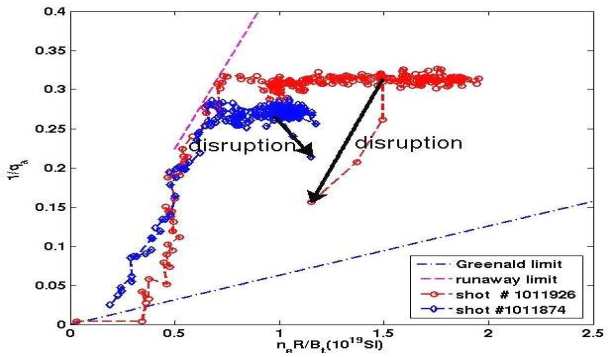

Fig. 8. The J-TEXT Hugill diagram with trajectories of two disruption events (J-TEXT shots 1011874 and 1011926, respectivelly), where the dash dotted line indicates the Greenwald density limit, the dashed line gives the runaway discharge limit. Here the low q limit above 0.45 is not shown in the plot.

J-TEXT is uniquely tolerant of disruptions and ideally suited for studies of a wide range of disruptive behavior: Low q, high density, MHD instability and mode locking, and other classes of disruption. In order to observe and catalogue the disruption events, J-TEXT is currently equipped with (1) AXUV arrays for the measurement of total radiation power, (2) Soft X-ray photodiode arrays for sawtooth oscillation, (3) 2D Mirnov coils for mode analysis, and (4) CIII and Hα for working gas and impurity flux.

During the J-TEXT early campaign (before Oct. 2009), some disruptions caused by high-m mode instability at very low current and density during the fast ramp-up phase could occur, but did little harm to the machine. Some other disruption events caused by the uncontrollable plasma displacement are also observed. Besides these cases, disruptions caused by low-m MHD mode instability and mode locking are currently more common in the J-TEXT operation. Under without auxiliary heating power and density modulation tools, MHD instability and locked modes could not be controlled and lead to the disruptions easily. Among 3500 shots (counted in the peroid of Oct. 2009-June 2010), 320 shots ended with a disruption. According to the statistical analysis of MHD events, disruptions caused by mode locking have a proportion of 24% of the disruption events, while the growth and saturation of pure m=2 tearing mode is another key cause of disruption and it contributes to 71% of the total value. The remaining 5% were caused by other unidentified effects. The descriptions below cover the two identified catagories of disruption generation, namely low-m MHD mode instability and mode locking.

Fig. 9 shows a typical example (J-TEXT shot 1011874) of how a disruption is triggered by mode locking. The corresponding trace of this shot is also given in the Hugill diagram (as shown in Fig. 8, denoted by open diamonds). In this discharge, the plasma current I_p reaches 200kA and the plasma density is about $2\times10^{19}m^{-3}$ during the flat-top. Therefore, the safety factor about 3.7 during the flat-top is far from the low-q limit, while the density is also far from the limit. All the characteristics reveal that this shot is located within the operation region. However, a disruption still occurs at t=2.105s. The results of variable-frequency complex demodulation applied to Mirnov coil signals shows that a MHD mode rotates at a frequency of 2kHz and lasting for a very long time till t=2.09s, just about 5ms before the hard X-ray signal step-up. At 2.095s (10ms before the current quench), the hard X-ray signal increase may imply that the plasma confinement begins to deteriorate, but other diagnostic signals do not have any obvious changes. During the period of 2.09-2.1s, the mode rotation starts to slow down gradually and completely lockes at the end. The mode inferred by phase analysis shows it is a m/n=2/1 tearing mode.

Fig. 10 gives other example (J-TEXT shot 1011926) of a disruption invoked by the increasing and saturation of m/n=2/1 tearing mode. The trace of this shot is also given in figure 8 (denoted by open circle) and confirms that the discharge stays within the operation region. But it still undergoes a soft disruption. In this discharge, the plasma density is above $3\times10^{19}m^{-3}$, so the mode is not easily locked due to the relatively high density. Fig. 10 displays the time evolution of diagnostic signals around the disruption. Since the perturbation field induces an increasing magnitude of m/n=2/1 mode at t=2.042s, the plasma confinement degrades. Therefore, the plasma density and intensity of Soft X-rays drop, and the loop voltage, CIII, Hα, and XUV signals step up slightly as well, which could be caused by the plasma-wall interaction. Abnormality in magnetic perturbation signals is seen during the time from t=2.042s to 2.057s. At t=2.058s, the discharge evolves into a disruption. The variable-frequency complex demodulation analysis indicates that the MHD mode is m/n=2/1 mode rotating at a frequency of 5kHz. The precursor phase in this shot is about 15ms, much longer than the case of mode locking shown in Fig. 9. For this type of disruption, the current profile is close to the marginal stability in the pre-precursor phase, so the MHD mode instability develops.

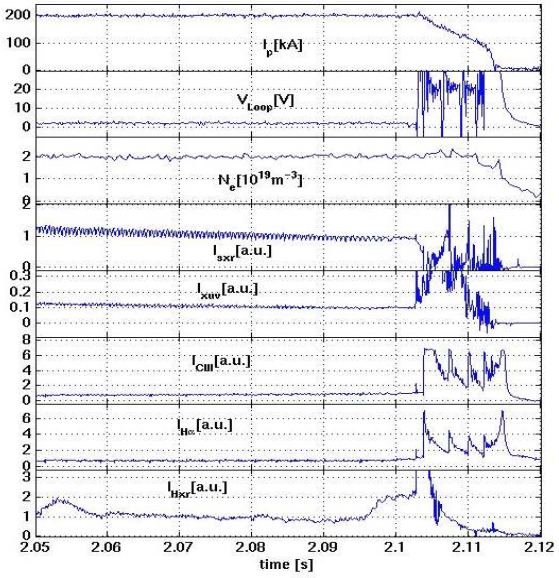

Fig. 9. The time evolution of diagnostic signals of J-TEXT shot 1011874 ended by a disruption caused by locked mode. (a) traces from the top to the bottom are plasma current, loop voltage, plasma density, intensity of soft X-rays, intensity of XUV, CIII amplitude, Hα amplitude, intensity of hard X-rays, respectively. (b) Mirnov pickup coil signal and the mode number inferred by phase analysis.

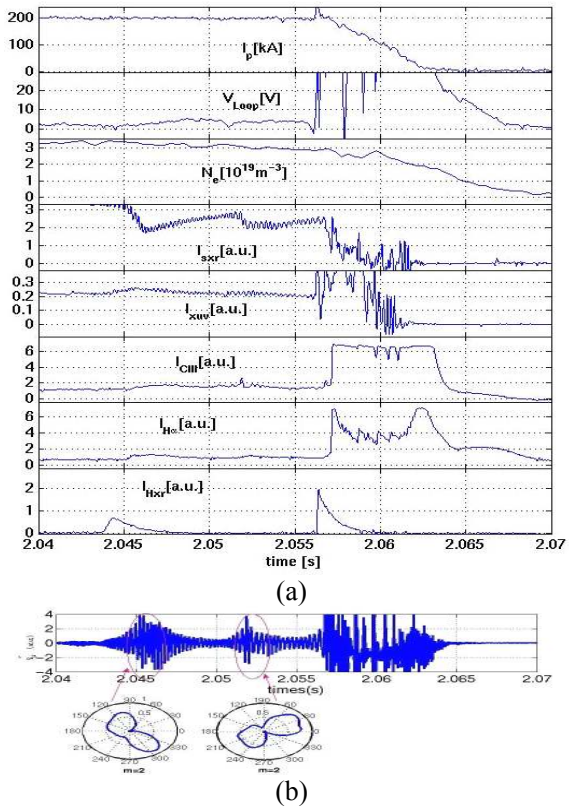

Fig. 10. The time evolution of diagnostic signals of J-TEXT shot 1011926 ended by a disruption caused by low-m MHD mode instability. (a) traces from the top to the bottom are plasma current, loop voltage, plasma density, intensity of soft X-rays, intensity of XUV, CIII amplitude, Hα amplitude, intensity of hard X-rays, respectively. (b) Mirnov pickup coil signal and the mode number inferred by phase analysis.

Those disruptions mentioned above occur under a normal or even higher density and

temperature conditions. For the low density discharges, there is a runaway limit found experimentally, as shown in Fig. 8. At present, the J-TEXT Ohmic discharges can reach a minimum density of $0.7\times10^{19}m^{-3}$. In the normal discharges located around the runaway limit, there are two abnormal cases observed. One is that the intensity of hard X-ray emission received from the radial direction increases accompanying a drop in the intensity from the tangential direction (referenced to the I_p direction). The other is that the plasma density and temperature slightly step up accompanying a hard X-rays increase in the tangential direction. The mechanisms for both cases are not so clear; more analysis is underway.

Furthermore, detailed studies of the disruption characteristics, including current spikes and other precursors of the thermal quench, various precursor mechanisms and the mechanism for the thermal quench, have been undertaken recently. For example, because of toroidal insulating gaps in the vacuum vessel of J-TEXT, the direct measurement of net currents in the shell is possible. The evidence of net currents inferred by comparing signals from the internal and external Rogowski coils is observed in some disruption events.

4. Future research plan

Apart from research progress already made, some projects relevant to the short-term research plan on the J-TEXT are going to launch this year: (1) Three sets of supersonic molecular beam injection (SMBI) systems with different injection angles will be set up to control the edge plasma density profile and to study the impurity transport. The completed electron density diagnostic devices with high spatial and temporal resolution will be useful for study of particle transport by SMBI and the oscillating gas puff technique. (2) A detailed study of the influence of resonant magnetic perturbations and/or stochastic magnetic fields on the MHD activity and heat and particle transport in the plasma edge region will start when the installation of Ergodic magnetic limiter and rotating magnetic field coils is completed. (3) A high resolution UV-visible spectrometer with good spatial resolution provided by a rotating mirror will be added for measurement of impurity transport on J-TEXT. (4) Two reciprocating Langmuir probes will be mounted on the top windows of the J-TEXT. They, together with numerous existing movable and fixed Langmuir probes, will be manipulated flexibly for edge turbulence studies. The study will concentrate on asymmetries and coherent structures across the LCFS. (5) A high-power 3-wave FIR laser polarimeter-interferometer used to provide the plasma current density profile will be built [15]. The measurement will enable a thorough investigation into the effect of the current density and its gradient on MHD events. (6) A 32-channel electron cyclotron emission (ECE) radiometer with high temporal and spatial resolution will be applied for J-TEXT temperature profile measurement. Its potential application to the study of thermal quench and to electron thermal transport in future with modulated ECH will be an interesting topic.

5. Summary

The TEXT-U tokamak, having been operated by the UT at Austin, was dismantled and shipped to China in 2004, and renamed as the Joint TEXT (J-TEXT). In 2007, the reconstruction of the machine was completed and the first plasma was obtained. The reconstruction of the J-TEXT tokamak not only included the assembly of the vacuum chamber, field coils, and iron core transformer, but also involved design and manufacture of pumping stations and gas puffing system, rebuilding the field coil power supplies, construction of the CCS system, establishment of the DAQ system, and so on. Moreover, a number of diagnostic systems used to facilitate the routine operation and research scenarios were developed.

Recently, the observation of MHD activity and preliminary analysis of disruption events were made. Measurements and analysis of the IBEs near the LCFS were also done. Apart from the reconstruction and research progress already made, some projects are going to launch this year, which includes setup of SMBI systems, resonance perturbation magnetic coils, UV-visible spectrometer, 3-wave FIR polarimeter-interferometer, and an ECE system. With those extensive modulation tools and diagnostic hardware being built, we will be able to carry out some thorough investigations into basic plasma physics processes. In a word, the machine is ready for productive research.

Acknowledgement

We are grateful to the help from the Southwestern Institute of Physics and the Institute of Plasma Physics, Chinese Academy of Science. This work is supported by the National 973 project of China (no. 2008CB717805).

References:

[1] UNIVERSITY OF TEXAS AT AUSTIN, Proposal for a fusion plasma research facility, Fusion Research Center, Austin (1976)
[2] UNIVERSITY OF TEXAS AT AUSTIN, The Texas Experimental Tokamak: a plasma research facility, DOE/ER/542/41-151, FRCR #470, Austin (1995)
[3] ZHUANG, G., DING, Y.H., et al, "Reconstruction of the TEXT-U Tokamak in China", Plasma Science and Technology 11 (2009) 439
[4] WESSON, J., Tokamaks, Oxford University Press, Cambridge (2004)
[5] DING, Y.H., ZHUANG, G., et al, "The vacuum system of the J-TEXT tokamak", Plasma Devices and Operations 17 (2009) 207
[6] ZHANG, M., ZHUANG, G., et al, "Design of the Control System of Toroidal Field (TF) Power Supply for J-TEXT Tokamak", Plasma Science and Technology 10 (2008) 754
[7] ZHANG, M., ZHUANG, G., et al, "The Power Supply System for the J-TEXT Poloidal Field", Plasma Science and Technology 11 (2009) 100
[8] YANG, Z.J., ZHUANG, G., et al, "Design and realization of the J-TEXT tokamak central control system", Fusion Engineering and Design 84 (2009) 2093
[9] QIU, S.S., ZHUANG, G., et al, "New PCB magnetic coils in the vacuum vessel of J-TEXT tokamak for position measurement", Rev. Sci. Instrum. (inpress)
[10] GAO, L., HU, X.W., et al, "The Microwave Interferometer on J-TEXT Tokamak", The 8th International Symposium on Antennas, Propagation, and EM Theory, Kunming (2008)
[11] ZHU, M., ZHUANG, G., et al, "A Visible Imaging System for the Estimation of Plasma Vertical Displacement in J-TEXT", Plasma Science and Technology (in press)
[12] DING, Y.H., ZHUANG, G., et al, "Soft x-ray imaging diagnostic system on the J-TEXT", Nuclear Instruments and Methods A 606 (2009) 743
[13] ZHANG, J., ZHUANG, G., et al, "A new absolute extreme ultraviolet image system designed for studying the radiated power of the Joint Texas Experimental Tokamak discharges", Rev. Sci. Instrum. 81 (2010) 073509
[14] ZHU, M., ZHUANG, G., et al, "Intermittency of the density fluctuations and its influence on the radial transport in the boundary of J-TEXT", Chinese Physics B (in press)
[15] CHEN, J., GAO, L., et al, "Design of a FIR three-wave polarimeter-interferometer system for J- TEXT Tokomak", Rev. Sci. Instrum. (in press)